

# Long-range string orders and topological quantum phase transitions in the one-dimensional quantum compass model

Hai Tao Wang<sup>1</sup> and Sam Young Cho<sup>1,\*</sup>

<sup>1</sup>*Centre for Modern Physics and Department of Physics,  
Chongqing University, Chongqing 400044, The People's Republic of China*

In order to investigate the quantum phase transition in the one-dimensional quantum compass model, we numerically calculate non-local string correlations, entanglement entropy, and fidelity per lattice site by using the infinite matrix product state representation with the infinite time evolving block decimation method. In the whole range of the interaction parameters, we find that the four distinct string orders characterize the four different Haldane phases and the topological quantum phase transition occurs between the Haldane phases. The critical exponents of the string order parameters  $\beta = 1/8$  and the central charges  $c = 1/2$  at the critical points show that the topological phase transitions between the phases belong to an Ising type of universality classes. In addition to the string order parameters, the singularities of the second derivative of the ground state energies per site, the continuous and singular behaviors of the von Neumann entropy, and the pinch points of the fidelity per lattice site manifest that the phase transitions between the phases are of the second-order, in contrast to the first-order transition suggested in previous studies.

PACS numbers: 75.10.Pq, 03.65.Vf, 03.67. Mn, 64.70.Tg

## I. INTRODUCTION

Transition metal oxides (TMOs) with orbital degeneracies have been intensively studied for quantum phase transitions (QPTs) because they have shown extremely rich phase diagrams due to competitions between orbital orderings and complex interplays between quantum fluctuations and spin interactions<sup>1-16</sup>. In order to mimic such competitions between orbital ordering in different directions and directional natures of the orbital states with twofold degeneracy in the language of the pseudospin-1/2 operators, Kugel and Khomskii<sup>17</sup> first introduced the quantum compass model (QCM) in 1973. In this model, the pseudospin-1/2 operators characterize the orbital degrees of freedom, and the anisotropic couplings between these pseudospins simulate the competition between orbital orderings in different directions. Furthermore, such an idea has been implemented to describe some Mott insulators with orbital degeneracy<sup>18,19</sup>, polar molecules in optical lattices<sup>20</sup> and ion trap systems<sup>21</sup>, protected qubits for quantum computation in Josephson junction arrays<sup>22</sup>, and so on.

Based on the one-dimensional QCM, physical properties and QPTs in TMOs have been explored in the absence<sup>1-7</sup> or in the presence<sup>8-13</sup> of a transverse magnetic field. Especially for its criticality, in 2007, Brzezicki *et al.*<sup>1</sup> used the Jordan-Wigner transformation mapping it to an Ising model, obtained an exact solution of the QCM, and suggested that the system has the first-order transition occurring between two disordered phases. In 2008, You and Tian<sup>2</sup> supported Brzezicki *et al.*'s result, i.e., the first-order transition by adopting the reflection positivity technique in the standard pseudospin representation. In 2009, in order to show that the phase transition is intrinsic to the system not an artifact originating from a singular parameterization of the exchange interactions, Brzezicki and Oleś<sup>3</sup> revisited the model and reclaimed the first-order transition. In the same year, furthermore, Sun *et al.*<sup>4</sup> reached to a conclusion supporting the first-order phase transition between two different disordered phases by using the fidelity suscep-

tibility and the concurrence. However, Sun and Chen<sup>8</sup> considered a transverse magnetic field on the QCM and found at the zero field that the phase transition is of the second-order from the finite-size scaling of the spin-spin correction as well as the fidelity susceptibility, the block entanglement entropy, and the concurrence. Also, following in Ref. 1 but introducing one more tunable parameter, Eriksson and Johannesson<sup>5</sup> noticed the second-order phase transition rather than the first-order phase transition by using the concurrence and the block entanglement at the multicritical point in the one-dimensional extended quantum compass model (EQCM). In 2012, Liu *et al.*<sup>7</sup> numerically studied the EQCM by utilizing the matrix product state (MPS) with the infinite time-evolving block decimation (iTEBD) algorithm and, at the multicritical point, observed both features of the first-order and the second-order phase transition. Thus, the phase transition in the one-dimensional QCM is still not characterized clearly.

It seems to be believed that the phase transition occurs between two disordered phases in the one-dimensional QCM. Normally, disordered phases are not characterized by any local order parameter. This implies that the phase transition in the one-dimensional QCM would not be understood properly within the Landau paradigm of spontaneous symmetry breaking<sup>23</sup>. Consequently, such a controversy on the phase transition in the one-dimensional QCM would suggest us to consider non-local long-range orders for its proper characterization. In order to characterize the phase transition properly, in this paper, we investigate non-local string orders in the one-dimensional QCM. Actually, a string order as a non-local long-range order was introduced by Nijs and Rommelse<sup>24</sup> and Tasaki<sup>25</sup>, and characterizes the Haldane phase in the spin-1 Heisenberg chain<sup>26</sup>. To calculate non-local string orders directly<sup>27</sup>, in contrast to an extrapolated value for finite-size lattices, we employ the infinite matrix product state (iMPS)<sup>28,29</sup> representation with the iTEBD algorithm developed by Vidal<sup>29</sup>. For a systematic study, the second derivative of ground state energy is calculated to reveal the phase transitions in the whole interaction parameter

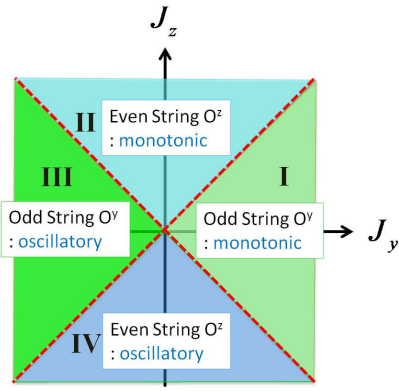


FIG. 1: (Color online) Groundstate phase diagram for the one-dimensional QCM in  $J_y$ - $J_z$  plane. The four topologically ordered phases are characterized by the four distinct string orders (defined in the text). The critical lines are (i)  $J_y = J_z > 0$  ( $\theta = \pi/4$ ), (ii)  $J_y = -J_z < 0$  ( $\theta = 3\pi/4$ ), (iii)  $J_y = J_z < 0$  ( $\theta = 5\pi/4$ ), and (iv)  $J_y = -J_z < 0$  ( $\theta = 7\pi/4$ ). At the critical points, the central charges are  $c = 1/2$  and the critical exponent of each string order is  $\beta = 1/8$ . The phase transitions between Haldane phases are a topological phase transition and belong to an Ising universality class. Here, the  $\theta$  is the interaction parameter from the setting  $J_y = J \cos \theta$  and  $J_z = J \sin \theta$  for the numerical calculation.

range. Its singularities indicate that there are the four phases separated by the second-order phase transitions. We find the four string order parameters that characterize each phase (see in Fig. 1), which means that all the four phases are a topologically ordered phase. Furthermore, the critical exponent from the string orders  $\beta = 1/8$  and the central charges  $c \approx 1/2$  at the critical points clarify that the topological quantum phase transitions (TQPTs) belong to the Ising-type phase transition. In addition, the continuous behaviors of the odd- and even-von Neumann entropies and the pinch points of the fidelity per lattice site (FLS) verify the second-order phase transitions between two topologically ordered phases.

This paper is organized as follows. In Sec. II, we introduce the one-dimensional QCM and discuss the second derivative of the ground state energy per site. In Sec. III, we display string correlations and define properly the four string order parameters characterizing the four topologically ordered phases. The critical exponents are presented. The phase transitions are discussed by employing the von Neumann entropy in Sec. IV. The TQPTs are classified based on the central charge via the finite-entanglement scaling. In Sec. V, we discuss the pinch points of the FLS. Finally, our conclusion is given in Sec. VI.

## II. QUANTUM COMPASS MODEL AND GROUNDSTATE ENERGY

We consider the one-dimensional spin-1/2 QCM<sup>1</sup> written as

$$H = \sum_{i=-\infty}^{\infty} \left( J_y S_{2i-1}^y \cdot S_{2i}^y + J_z S_{2i}^z \cdot S_{2i+1}^z \right), \quad (1)$$

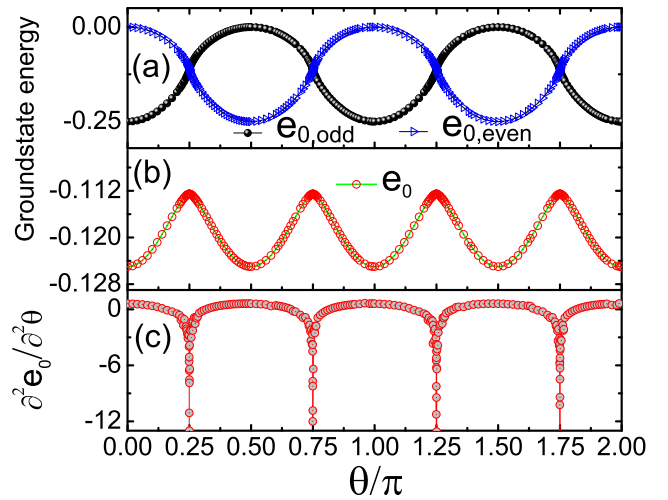


FIG. 2: (Color online) (a) Groundstate energies per site on odd/even-bonds  $e_{0,odd/even}$ , (b) average energy  $e_0 = (e_{0,odd} + e_{0,even})/2$ , and (c) second derivative of the average energy  $e_0$  as a function of the interaction parameter  $\theta$ . Here, the truncation dimension  $\chi = 40$  is chosen for the iMPS calculation. In (c), note that the singular behaviors of the second derivative occur at the points  $\theta = \pi/4$ ,  $\theta = 3\pi/4$ ,  $\theta = 5\pi/4$ , and  $\theta = 7\pi/4$ .

where  $S_i^y$  and  $S_i^z$  are the spin-1/2 operators on the  $i$ th site.  $J_y$  and  $J_z$  are nearest-neighbor exchange couplings on the odd and the even bonds, respectively. In order to cover the whole range of the parameter  $J_y$  and  $J_z$ , we set  $J_y = J \cos \theta$  and  $J_z = J \sin \theta$ .

From the iMPS groundstate wavefunction, we obtain the groundstate energy of the QCM. In Figs. 2(a) and 2(b), we plot the groundstate energies  $e_{0,odd}$  on the odd bond and  $e_{0,even}$  on the even bond, and the groundstate energy per site  $e_0$  as an average value of the energies  $e_{0,odd}$  and  $e_{0,even}$ , i.e.,  $e_0 = (e_{0,odd} + e_{0,even})/2$ . Here, the truncation dimension is chosen as  $\chi = 40$ . The energies are shown to be a periodic behavior as a function of the interaction parameter  $\theta$ . One way to know whether there is a phase transition is to check the non-analyticity of the groundstate energy on the system parameters. Thus, in order to see any possible phase transition, we calculate the derivative of the energies over the interaction parameter  $\theta$ . In the first derivative of the energies over the interaction parameter, no singular behavior is noticed in the whole parameter range. Then, in Fig. 2(c), we plot the second derivative of the energy  $e_0$ . Note that it exhibits the singular points at  $\theta = \pi/4$ ,  $\theta = 3\pi/4$ ,  $\theta = 5\pi/4$ , and  $\theta = 7\pi/4$ . This result means that, at the singular points, the quantum phase transitions occur and they are of the second-order. As we introduced the controversy of the phase transition in the QCM, the critical point  $\theta = \pi/4$  in our calculation corresponds to the critical point  $J_y = J_z$  investigated in previous studies. Consequently, our second derivative of the groundstate energy shows that the phase transition in the QCM should be of the second-order. Moreover, the critical lines separate the parameter space into the four regions [denoted by I, II, III, and IV in Fig. 1], which may indicate four possible phases. Then,

in order to characterize the four possible phases, we discuss string correlations in the next section.

### III. STRING ORDER PARAMETERS AND TOPOLOGICAL QUANTUM PHASE TRANSITIONS

The QCM has the different strengths of the spin exchange interaction depending on the odd and the even bonds. One can then define string correlations based on the bond alternation<sup>30,31</sup>. Let us first consider the string correlations defined as

$$O_{s,odd}^\alpha(2i-1, 2j) = \left\langle S_{2i-1}^\alpha \exp \left[ i\pi \sum_{k=2i}^{2j-1} S_k^\alpha \right] S_{2j}^\alpha \right\rangle \quad (2a)$$

$$O_{s,even}^\alpha(2i, 2j+1) = \left\langle S_{2i}^\alpha \exp \left[ i\pi \sum_{k=2i+1}^{2j} S_k^\alpha \right] S_{2j+1}^\alpha \right\rangle, \quad (2b)$$

where  $\alpha = x, y,$  and  $z$ . We observe numerically that the  $x$  components of the string correlations  $O_{str,odd/even}^x$  decrease to zero within the lattice distance  $|i-j| = 6$  in the whole parameter range.

*Behaviors of odd string correlations.*— In Fig. 3(a), we summarize the short- and long-distance behaviors of the odd string correlations  $O_{str,odd}^y$  in  $J_y$ - $J_z$  plane. (i) For  $|J_y| < |J_z|$  (the regions II and IV in Fig. 1), the odd string correlations  $O_{str,odd}^{y/z}$  decrease to zero within the lattice distance  $|i-j| = 80$ . (ii) For  $|J_y| > |J_z|$  (the regions I and III in Fig. 1), the absolute value of  $O_{str,odd}^y$  are saturated to a finite value while  $O_{str,odd}^z$  decays to zero very slowly, which means  $O_{str,odd}^y$  as a non-local long-range order parameter [indicated by the asterisk in Fig. 3(a)] can characterize a topologically ordered phase. Further, if  $J_y > 0$  [region I] ( $J_y < 0$  [region III]),  $O_{str,odd}^y$  shows a monotonic (oscillatory) saturation and  $O_{str,odd}^z$  displays an oscillatory (monotonic) decaying to zero.

As an example, in Fig. 3(b), we plot the odd string correlations  $O_{str,odd}^{y/z}$  as a function of the lattice distance  $|i-j|$  for  $\theta = 0.2\pi$  (the range I) and  $\theta = 0.8\pi$  (the region III). The string correlations are shown a very distinct behavior. For  $\theta = 0.2\pi$ , the  $O_{str,odd}^y$  has a minus sign, while the  $O_{str,odd}^z$  has an alternating sign depending on the lattice distance. In contrast to the case of  $\theta = 0.2\pi$ , for  $\theta = 0.8\pi$ , the  $O_{str,odd}^z$  has a minus sign, while the  $O_{str,odd}^y$  has an alternating sign depending on the lattice distance. From the short-distance behaviors, as shown in Fig. 3(b), it is hard to see whether the string correlations decay to survive in the long distance limit (i.e.,  $|i-j| \rightarrow \infty$ ). In order to study the correlations in the limit of the infinite distance, one can then set a truncation error  $\varepsilon$  rather than the lattice distance, i.e.,  $O(|i-j|) - O(|i-j-1|) < \varepsilon$ . In this study, for instance,  $\varepsilon = 10^{-8}$  is set. The insets of Fig. 3(b) show the string correlations for relatively very large lattice distance. We see clearly that the  $O_{str,odd}^y$ 's have a finite value while the  $O_{str,odd}^z$ 's decay to zero (around the lattice distance  $|i-j| \sim 5 \times 10^4$ ). As a consequence, the parameter regions I and III can be characterized by the odd string long-range order parameters. As discussed above, the odd string

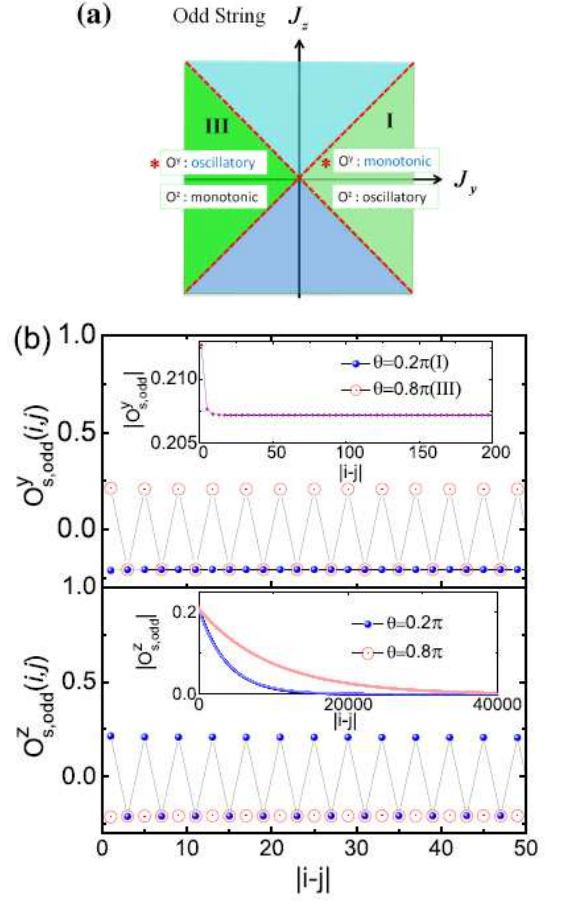


FIG. 3: (Color online) (a) Behaviors of the odd string order parameters (indicated by the asterisk) in  $J_y$ - $J_z$  plane. (b) String correlations  $O_{str,odd}^{y/z}$  for  $\theta = 0.2\pi$  and  $\theta = 0.8\pi$ . In the insets, note that  $O_{str,odd}^y$ 's are saturated to a finite value, while  $O_{str,odd}^z$ 's decay to zero for very large distance.

correlations have the two characteristic behaviors, i.e., one is a monotonic saturation for  $\theta = 0.2\pi$ , the other is an oscillatory saturation for  $\theta = 0.8\pi$ . Such a distinguishable behavior of the string correlations allows us to say that the region I ( $J_y > 0$ ) and the region III ( $J_y < 0$ ) are a different phase each other and we call the *monotonic* odd string order and the *oscillatory* odd string order, respectively.

*Behaviors of even string correlations.*— Similarly to the odd string correlations, the even string correlations show the two characteristic behaviors. In Fig. 4(a), we summarize the short- and long-distance behaviors of the even string correlations  $O_{str,even}^y$  in  $J_y$ - $J_z$  plane. (i) For  $|J_z| < |J_y|$  (the regions I and III in Fig. 1), the even string correlations  $O_{str,even}^{y/z}$  decrease to zero within the lattice distance  $|i-j| = 80$ . (ii) For  $|J_z| > |J_y|$  (the regions II and IV in Fig. 1), the absolute value of  $O_{str,even}^z$  are saturated to a finite value while  $O_{str,even}^y$  decays to zero very slowly, which means  $O_{str,even}^z$  as a non-local long-range order parameter [indicated by an asterisk in Fig. 4(a)] characterizes a topologically ordered phase. Further, if  $J_z > 0$  [region II] ( $J_z < 0$  [region IV]),  $O_{str,even}^z$  shows a monotonic (oscillatory)

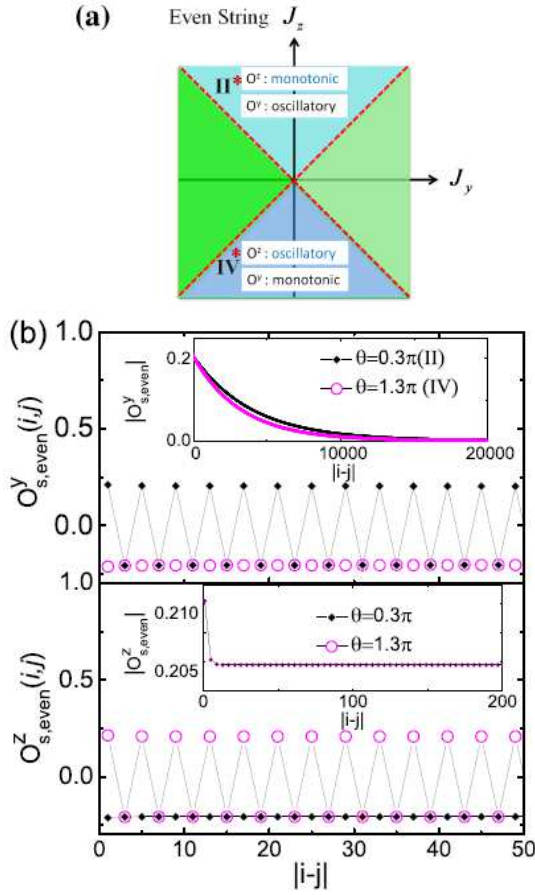


FIG. 4: (Color online) (a) Behaviors of the even string order parameters (indicated by the asterisk) in  $J_y$ - $J_z$  plane. (b) String correlations  $O_{str,even}^{y/z}$  for  $\theta = 0.3\pi$  and  $\theta = 1.3\pi$ . In the insets, note that  $O_{str,even}^z$ 's are saturated to a finite value, while  $O_{str,even}^y$ 's decay to zero for very large distance.

saturation and  $O_{str,even}^y$  displays an oscillatory (monotonic) decaying to zero.

As an example, in Fig. 4(b), we plot the even string correlations  $O_{str,even}^{y/z}$  as a function of the lattice distance  $|i-j|$  for  $\theta = 0.3\pi$  (the range II) and  $\theta = 1.3\pi$  (the region IV). For  $\theta = 0.3\pi$ , the  $O_{str,even}^y$  has an alternating sign depending on the lattice distance, while the  $O_{str,even}^z$  has a minus sign. In contrast to the case of  $\theta = 0.3\pi$ , for  $\theta = 1.3\pi$ , the  $O_{str,even}^z$  has an alternating sign depending on the lattice distance, while the  $O_{str,even}^y$  has a minus sign. Similarly to the odd string correlations, the short distance behaviors of the even string correlations show to the difficulty to see which the string correlations survive in the long distance limit (i.e.,  $|i-j| \rightarrow \infty$ ). By using the truncation error  $\varepsilon = 10^{-8}$ , we plot the string correlations for relatively very large lattice distance in the insets of Fig. 4(b). We see clearly that the  $O_{str,even}^z$ 's have a finite value while the the  $O_{str,even}^y$ 's decay to zero (around the lattice distance  $|i-j| \sim 2 \times 10^4$ ). As a result, the parameter regions II and IV can be characterized by the even string long-range order parameters. The even string correlations also have the two

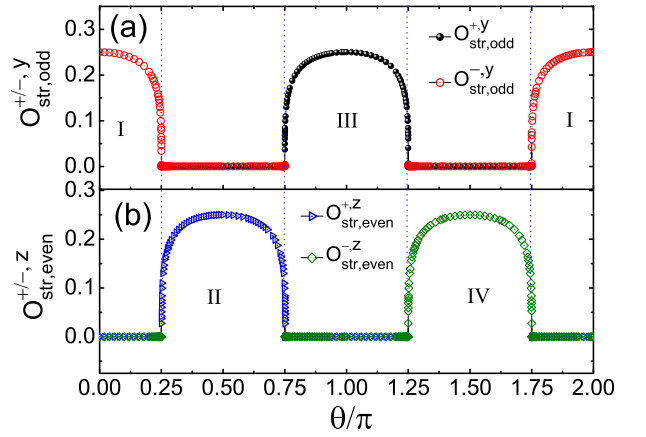


FIG. 5: (Color online) String order parameters (a)  $O_{str,odd}^{+/-,y}$  and (b)  $O_{str,even}^{+/-,z}$  as a function of  $\theta$ . The order parameters are defined in the text.

characteristic behaviors, i.e., one is a monotonic saturation for  $\theta = 0.3\pi$ , the other is an oscillatory saturation for  $\theta = 1.3\pi$ . The region II ( $J_z > 0$ ) and the region IV ( $J_z < 0$ ) are a different phase each other and we call the *monotonic* even string order and the *oscillatory* even string order, respectively.

*Phase diagram from string order parameters.*— As we discussed, the even and odd string correlations have shown two characteristic behaviors, i.e., one is monotonic, the other is oscillatory. Then, one may define a proper long-range order based on the behaviors of the odd and the even string correlations. We define the long-range string order parameters as follows:

$$O_{str,odd}^{+,y} = - \lim_{|i-j| \rightarrow \infty} O_{s,odd}^y(2i-1, 2j), \quad (3a)$$

$$O_{str,odd}^{-,y} = - \lim_{|i-j| \rightarrow \infty} (-1)^{(j-i+1)} O_{s,odd}^y(2i-1, 2j), \quad (3b)$$

$$O_{str,even}^{+,z} = - \lim_{|i-j| \rightarrow \infty} O_{s,even}^z(2i, 2j+1), \quad (3c)$$

$$O_{str,even}^{-,z} = - \lim_{|i-j| \rightarrow \infty} (-1)^{(j-i+1)} O_{s,even}^z(2i, 2j+1), \quad (3d)$$

where, actually, the superscript + (-) of the string order parameters denotes the monotonic behavior (the oscillatory behavior).

The defined string orders are calculated from the iMPS groundstate wave function. In Fig. 5, we display the string order parameters as a function of the interaction parameter  $\theta$ . In Fig. 5(a), it is clearly shown that the odd string order parameters are finite for the region I ( $-\pi/4 < \theta < \pi/4$ ) and the region III ( $3\pi/4 < \theta < 5\pi/4$ ). Further, the monotonic odd string order parameter  $O_{str,odd}^{+,y}$  characterizes the region I and the oscillatory odd string order parameter  $O_{str,odd}^{-,y}$  does the region III. Similarly to the odd string order parameters, the  $z$  components of the even string order parameters  $O_{str,even}^{+,z}$  and  $O_{str,even}^{-,z}$  are finite for the region II ( $\pi/4 < \theta < 3\pi/4$ ) and the region IV ( $5\pi/4 < \theta < 7\pi/4$ ). The monotonic even string order parameter  $O_{str,even}^{+,z}$  characterizes the region II and the oscillatory even string order parameter  $O_{str,even}^{-,z}$  does the region IV. Consequently, the four regions in  $J_y$ - $J_z$  plane [Fig. 1] are character-

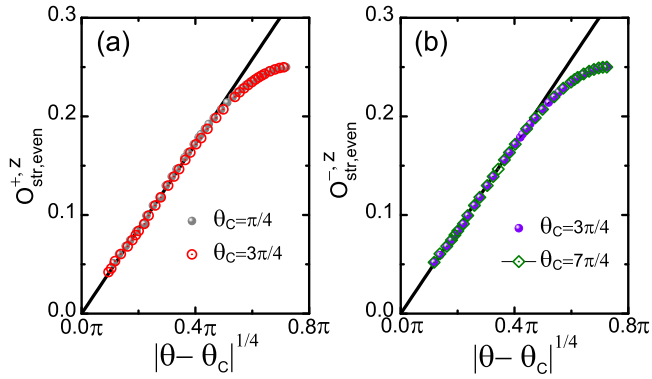


FIG. 6: (Color online) String order parameters (a)  $O_{str,even}^{+,z}$  and (b)  $O_{str,even}^{-,z}$  as a function of  $|\theta - \theta_c|^{1/4}$  for  $\theta_c = \pi/4, 3\pi/4, 5\pi/4,$  and  $7\pi/4$ .

ized by the four string order parameters  $O_{str,odd}^{+/-,y}$  and  $O_{str,even}^{+/-,z}$ , respectively, which implies that a different hidden  $Z_2 \times Z_2$  breaking symmetry occurs in each phase. Therefore, the one-dimensional QCM has the four distinct topologically ordered phases rather than disordered phases suggested in previous studies. The system undergoes a topological quantum phase transition between two topological ordered phases as the interaction parameter crosses the critical lines  $|J_y| = |J_z|$ . In addition, the continuous behaviors of the string order parameters across the critical lines show that the topological quantum phase transitions are of the continuous (second-order) phase transition rather than the discontinues (first-order) phase transition.

In a previous study<sup>7</sup> on an EQCM, the existence of a string order has been noticed numerically for a relevant interaction parameter range. However, any characterization of phase has not been made in association with the one-dimensional QCM. However, the one-dimensional spin-1/2 Kitaev model<sup>32</sup>, which is equivalent to the one-dimensional QCM, has shown to have two string order parameters<sup>33</sup> based on the dual spin correlation function<sup>34</sup> by using a dual transformation<sup>35,36</sup> mapping the model into a one-dimensional Ising model with a transverse field. The actual parameter range in the one-dimensional Kitaev model studied in Ref. 33 corresponds to  $J_y > 0$  and  $J_z > 0$  in our one-dimensional QCM. The system was discussed to undergo a topological quantum phase transition at the critical point  $J_y = J_z > 0$  ( $\theta = \pi/4$ ). In this sense, in the case of  $J_y, J_z > 0$  in the one-dimensional QCM, we have numerically demonstrated and verified the existence of the string order parameters and the topological quantum phase transition as discussed in Ref. 33.

*Critical exponents.*— In the critical regimes, as the order parameters, the string orders should show a scaling behavior to characterize the phase transitions. We plot the string order parameters  $O_{str,even}^{+,z}$  [Fig. 6(a)] and  $O_{str,even}^{-,z}$  [Fig. 6(b)] as a function of  $|\theta - \theta_c|^{1/4}$  with the critical points  $\theta_c = \pi/4, 3\pi/4, 5\pi/4,$  and  $7\pi/4$ . It is shown that all the string order parameters nearly collapse onto one scaling fitting function in the critical regimes, i.e., they scales as  $O_{str,even/odd}^{\pm,z/y} \propto |\theta - \theta_c|^{1/4}$ . As a result, the same critical exponents are given as  $\beta = 1/8$  via

$O_{str,even}^{+/-,z} \propto |\theta - \theta_c|^{2\beta^{37}}$ , which reveals that the TQPTs belong to the Ising-type phase transition.

#### IV. ENTANGLEMENT ENTROPY AND CENTRAL CHARGE

Quantum entanglement in many-body systems can be quantified by the von Neumann entropy that is a good measure of bipartite entanglement between two subsystems of a pure state<sup>38,39</sup>. Generally, for one-dimensional quantum spin lattices, at critical points, the von Neumann entropy exhibits its logarithmic scaling conforming conformal invariance. Its scaling is governed by a universal factor, i.e., a central charge  $c$  of the associated conformal field theory. The central charge allows us to classify a universality class<sup>40</sup> of quantum phase transition. In our iMPS representation, a diverging entanglement at quantum critical points gives simple scaling relations for (i) the von Neumann entropy  $S$  and (ii) a correlation length  $\xi$  with respect to the truncation dimension  $\chi$ <sup>41</sup> as follows:

$$\xi(\chi) \propto \xi_0 \chi^\kappa \quad (4a)$$

$$S(\chi) \propto \frac{c\kappa}{6} \log_2 \chi, \quad (4b)$$

where  $\kappa$  is a so-called finite-entanglement scaling exponent and  $\xi_0$  is a constant. Thus, one can calculate a central charge by using Eqs. (4a) and (4b).

In order to obtain the von Neumann entropy, we partition the spin chain into the two parts denoted by the left semi-infinite chain  $L$  and the right semi-infinite chain  $R$ . In terms of the reduced density matrix  $\rho_L$  or  $\rho_R$  of the subsystems  $L$  and  $R$ , the von Neumann entropy can be defined as  $S = -\text{Tr} \rho_L \log_2 \rho_L = -\text{Tr} \rho_R \log_2 \rho_R$ .

In the iMPS representation, the iMPS groundstate wavefunction can be written by the Schmidt decomposition  $|\Psi\rangle = \sum_{\alpha=1}^{\chi} \lambda_{\alpha} |\phi_{\alpha}^L\rangle |\phi_{\alpha}^R\rangle$ , where  $|\phi_{\alpha}^L\rangle$  and  $|\phi_{\alpha}^R\rangle$  are the Schmidt bases for the semi-infinite chains  $L(-\infty, \dots, i)$  and  $R(i+1, \dots, \infty)$ , respectively.  $\lambda_{\alpha}^2$  are actually eigenvalues of the reduced density matrices for the two semi-infinite chains  $L$  and  $R$ . In our four-site translational invariant iMPS representation, we have the four Schmidt coefficient matrices  $\lambda_A, \lambda_B, \lambda_C$  and  $\lambda_D$ , which means that there are the four possible ways for the partitions. Due to the two-site translational invariance of the QCM, in fact, we have  $\lambda_A = \lambda_C$  and  $\lambda_B = \lambda_D$ , i.e., one partition is on the odd sites, the other is on the even sites. From the  $\lambda_{even}$  and  $\lambda_{odd}$ , one can obtain the two von Neumann entropies depending on the odd- or even-site partitions as

$$S_{even/odd} = - \sum_{\alpha=1}^{\chi} \lambda_{even/odd,\alpha}^2 \log_2 \lambda_{even/odd,\alpha}^2, \quad (5)$$

where  $\lambda_{even/odd,\alpha}$ 's are diagonal elements of the matrix  $\lambda_{even/odd}$ .

In Fig. 7(a), we plot the von Neumann entropies  $S_{odd}(\theta)$  and  $S_{even}(\theta)$  as a function of the control parameter  $\theta$ . One can easily notice that there are the four singular points  $\theta = \pi/4, 3\pi/4, 5\pi/4,$  and  $7\pi/4$  in both the odd-bond and the even-bond entropies. The four singular points of the von Neumann

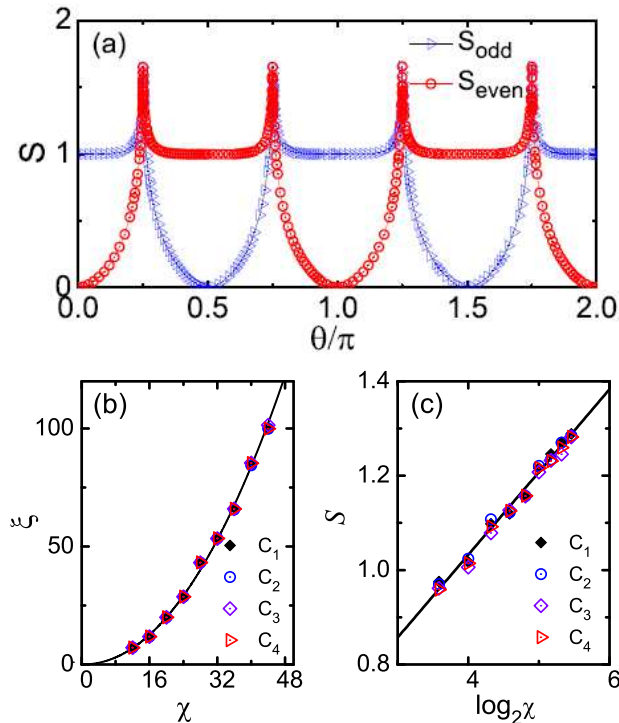


FIG. 7: (Color online) Von Neumann entropies  $S_{\text{odd}}$  and  $S_{\text{even}}$  as a function of the interaction parameter  $\theta$ . Note that the entropy singular points at  $\theta = \pi/4, 3\pi/4, 5\pi/4$ , and  $7\pi/4$  correspond to the critical points from the string order parameters. (b) Correlation length  $\xi(\chi)$  as a function of the truncation dimension  $\chi$  at the critical points  $C_1(J_x, J_y) = (1, 1)$ ,  $C_2 = (-1, 1)$ ,  $C_3 = (-1, -1)$ , and  $C_4 = (1, -1)$ . (c) Von Neumann entropy  $S(\chi)$  as a function of  $\chi$  at the critical points.

entropies indicate a quantum phase transition at those points. It should be noted that the detected transition points from the von Neumann entropies correspond to the critical points from the second derivative of the groundstate energy and the string order parameters. The continuous behaviors of von Neumann entropies around critical points also indicate the occurrence of the continuous (second-order) quantum phase transition as the system crosses the transition points. Hence, it is shown that the von Neumann entropy can detect the topological quantum phase transitions.

In Figs. 7(b) and 7(c), we plot the correlation length  $\xi(\chi)$  as a function of the truncation dimension  $\chi$  and the von Neumann entropy  $S(\chi)$  as a function of  $\chi$  at the critical points  $C_1(J_1, J_2) = (1, 1)$ ,  $C_2 = (-1, 1)$ ,  $C_3 = (-1, -1)$ , and  $C_4 = (1, -1)$ , respectively. The truncation dimensions are taken as  $\chi = 12, 16, 20, 24, 28, 32, 40$ , and  $44$ . The correlation length  $\xi(\chi)$  and the von Neumann entropy  $S(\chi)$  diverge as the truncation dimension  $\chi$  increases. Using the numerical fitting function  $\xi(\chi) = \xi_0 \chi^\kappa$  in Eq. (4a), the fitting constants are obtained as (i)  $\xi_0 = 0.04$  and  $\kappa = 2.071$  at  $C_1$ , (ii)  $\xi_0 = 0.041$  and  $\kappa = 2.068$  at  $C_2$ , (iii)  $\xi_0 = 0.039$  and  $\kappa = 2.087$  at  $C_3$ , and (iv)  $\xi_0 = 0.041$  and  $\kappa = 2.065$  at  $C_4$ . In order to obtain the central charge, we use the numerical fitting function of the von Neumann entropy  $S(\chi) = (c\kappa/6) \log_2 \chi + S_0$ . As shown in

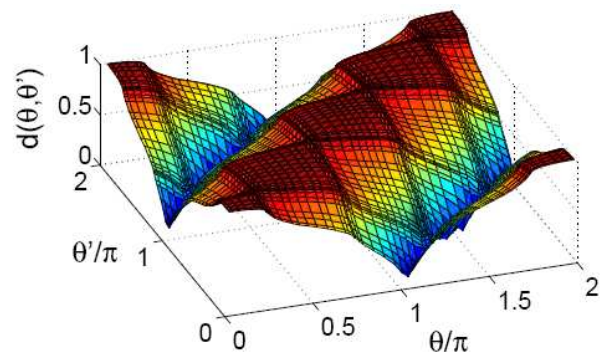


FIG. 8: (Color online) Fidelity per site  $d(\theta, \theta')$  surface as a function of the two parameters  $\theta$  and  $\theta'$ . The pinch points  $\theta = \pi/4, 3\pi/4, 5\pi/4$ , and  $7\pi/4$  on the FLS surface indicate the occurrence of the continuous phase transitions.

Figs. 7(c), the linear scaling behaviors of the entropies give (i)  $c = 0.5079$  with  $S_0 = 0.331$  at  $C_1$ , (ii)  $c = 0.4992$  with  $S_0 = 0.3464$  at  $C_2$ , (iii)  $c = 0.5048$  with  $S_0 = 0.314$  at  $C_3$ , and (iv)  $c = 0.5983$  with  $b = 0.34$  at  $C_4$ . Our central charges are very close to the value  $c = 0.5$ , respectively. Consequently, the topological quantum phase transitions at all the critical points belong to the same universality class, i.e., the Ising universality class. This result is consistent with the universality class from the critical exponent  $\beta = 1/8$  of the string order parameters.

## V. FIDELITY PER LATTICE SITE

Similarly to the von Neumann entropy, the fidelity per lattice site (FLS)<sup>42</sup> is known to enable us to detect a phase transition point as an universal indicator without knowing any order parameters. From our iMPS groundstate wave function  $|\Psi(\theta)\rangle$  with the interaction parameter  $\theta$ , we define the fidelity as  $F(\theta, \theta') = |\langle \Psi(\theta) | \Psi(\theta') \rangle|$ . Following Ref. 42, the groundstate FLS  $d(\theta, \theta')$  can then be defined as

$$\ln d(\theta, \theta') = \lim_{L \rightarrow \infty} \frac{\ln F(\theta, \theta')}{L}, \quad (6)$$

where  $L$  is the system size.

In Fig. 8, the groundstate FLS  $d(\theta, \theta')$  is plotted in  $\theta$ - $\theta'$  parameter space. The FLS surface reveals that there are the four pinch points  $\theta = \pi/4, 3\pi/4, 5\pi/4$ , and  $7\pi/4$ . Each pinch point corresponds to each phase transition point from the second-order derivative of the ground-state energy, the string order parameters, and the von Neumann entropy. In addition, the continuous behavior of the groundstate FLS verifies that the second-order quantum phase transitions occur at the pinch points.

## VI. CONCLUSION

We have investigated the quantum phase transition in the one-dimensional QCM by using the iMPS representation with

the iTEBD algorithm. To characterize quantum phases in the one-dimensional QCM, we introduced the odd and the even string correlations based on the alternating strength of the exchange interaction. We have observed that there are the two distinct behaviors of the odd and the string correlations, i.e., one is of the monotonic, (ii) the other is of the oscillatory. Based on the topological characterization, we find that there are the four topologically ordered phases in the whole interaction parameter range [Fig. 1]. In the critical regimes, the critical exponents of the string order parameters are obtained as  $\beta = 1/8$ , which implies that the topological quantum phase transitions belong to the Ising type of universality class. Consistently, we obtain the central charges  $c = 1/2$  from the entanglement entropy. In addition, the singular behaviors of the second-order derivatives of ground state energy,

the string order parameters characterizing the four Haldane phases, the continuous behaviors of the von Neumann entropy and the FLS allow us to conclude that the phase transitions in the one-dimensional QCM are of the second-order, in contrast to previous studies.

### Acknowledgments

We thank Huan-Qiang Zhou for useful comments. HTW acknowledges a support by the National Natural Science Foundation of China under the Grant No. 11104362. The work was supported by the National Natural Science Foundation of China under the Grants No. 11374379.

- 
- \* Electronic address: sycho@cqu.edu.cn
- <sup>1</sup> W. Brzezicki, J. Dziarmaga, and A. M. Oleś, Phys. Rev. B **75**, 134415 (2007).
  - <sup>2</sup> W. L. You and G. S. Tian, Phys. Rev. B **78**, 184406 (2008).
  - <sup>3</sup> W. Brzezicki and A. M. Oleś, Acta Phys. Polon. A **115**, 162 (2009).
  - <sup>4</sup> K.-W. Sun, Y.-Y. Zhang, and Q.-H. Chen, Phys. Rev. B **79**, 104429 (2009).
  - <sup>5</sup> E. Eriksson and H. Johannesson, Phys. Rev. B **79**, 224424 (2009).
  - <sup>6</sup> S. Mahdaviifar, Eur. Phys. J. B **77**, 77 (2010).
  - <sup>7</sup> G. H. Liu, W. Li, W. L. You, G. S. Tian, and G. Su, Phys. Rev. B **85**, 184422 (2012).
  - <sup>8</sup> K.-W. Sun and Q.-H. Chen, Phys. Rev. B **80**, 174417 (2009).
  - <sup>9</sup> L. C. Wang and X. X. Yi, Eur. Phys. J. D **77**, 281 (2010).
  - <sup>10</sup> R. Jafari, Phys. Rev. B **84**, 035112 (2011).
  - <sup>11</sup> M. Motamedifar, S. Mahdaviifar, and S. Farjami Shayesteh, Eur. Phys. J. B **83**, 181 (2011).
  - <sup>12</sup> W. L. You, Eur. Phys. J. B **85**, 83 (2012).
  - <sup>13</sup> G. H. Liu, W. Li, and W. L. You, Eur. Phys. J. B **85**, 168 (2012).
  - <sup>14</sup> S. Wenzel and W. Janke, Phys. Rev. B **78**, 064402 (2008).
  - <sup>15</sup> Orús R, A. C. Doherty, and G. Vidal, Phys. Rev. Lett. **102**, 077203 (2009).
  - <sup>16</sup> G. Jackeli and G. Khaliullin, Phys. Rev. Lett. **102**, 017205 (2009).
  - <sup>17</sup> K. I. Kugel and D. I. Khomskii, Zh. Eksp. Teor. Fiz. **64**, 1429 (1973) [Sov. Phys. JETP **37**, 725 (1973)].
  - <sup>18</sup> L. F. Feiner, A. M. Oleś, and J. Zaanen, Phys. Rev. Lett. **78**, 2799 (1997).
  - <sup>19</sup> J. Dorier, F. Becca, and F. Mila, Phys. Rev. B **72**, 024448 (2005).
  - <sup>20</sup> A. Micheli, K. G. Brennan, and Zoller, Nature Phys. **2**, 341 (2006).
  - <sup>21</sup> P. Milman, W. Mainault, S. Guibal, B. Doucot, L. Ioffe, and T. Coudreau, Phys. Rev. Lett. **99**, 020503 (2007).
  - <sup>22</sup> B. Doucot, M. V. Feigelman, L. B. Ioffe, and A. S. Iosevich, Phys. Rev. B **71**, 024505 (2005).
  - <sup>23</sup> S. Sachdev, *Quantum Phase Transition* (Cambridge University Press, Cambridge, 1999).
  - <sup>24</sup> M. den Nijs and K. Rommelse, Phys. Rev. B **40**, 4709 (1989).
  - <sup>25</sup> H. Tasaki, Phys. Rev. Lett. **66**, 798 (1991).
  - <sup>26</sup> S. Yamamoto, Phys. Rev. B **55**, 3603 (1997).
  - <sup>27</sup> Y. H. Su, S. Y. Cho, B. Li, H.-L. Wang, and H.-Q. Zhou, J. Phys. Soc. Jpn. **81**, 074003 (2012).
  - <sup>28</sup> G. Vidal, Phys. Rev. Lett. **91**, 147902 (2003).
  - <sup>29</sup> G. Vidal, Phys. Rev. Lett. **98**, 070201 (2007).
  - <sup>30</sup> K. Hida, Phys. Rev. B **45**, 2207 (1992).
  - <sup>31</sup> H. T. Wang, B. Li, and S. Y. Cho, Phys. Rev. B **87**, 054402 (2013).
  - <sup>32</sup> A. Y. Kitaev, Ann. Phys. (N.Y.) **303**, 2 (2003).
  - <sup>33</sup> X.-Y. Feng, G.-M. Zhang, and T. Xiang, Phys. Rev. Lett. **98**, 087204 (2007).
  - <sup>34</sup> P. Pteuty, Ann. Phys. (N.Y.) **57**, 79 (1970).
  - <sup>35</sup> E. Fradkin and L. Susskind, Phys. Rev. D **17**, 2637 (1978).
  - <sup>36</sup> M. Kohmoto and H. Tasaki, Phys. Rev. B **46**, 3486 (1992).
  - <sup>37</sup> D. G. Shelton, A. A. Nersisyan, and A. M. Ysvelik, Phys. Rev. B **53**, 8521 (1996).
  - <sup>38</sup> A. Osterloh, L. Amico, G. Falci, and R. Fazio, Nature (London) **416**, 608 (2002).
  - <sup>39</sup> L. Amico, R. Fazio, A. Osterloh, and V. Vedral, Rev. Mod. Phys. **80**, 517 (2008).
  - <sup>40</sup> P. Calabrese and J. Cardy, J. Phys. A: Math. Theor. **42**, 504005 (2009); J. Cardy, *Scaling and Renormalization in Statistical Physics*, (Oxford, University of Oxford, 1996).
  - <sup>41</sup> L. Tagliacozzo, T. R. de Oliveira, S. Iblisdir and J. I. Latorre, Phys. Rev. B **78**, 024410 (2008); F. Pollmann, S. Mukerjee, A. Turner and J. E. Moore, Phys. Rev. Lett. **102**, 255701 (2009); G. Vidal, J. I. Latorre, E. Rico and A. Kitaev, Phys. Rev. Lett. **90**, 227902 (2003).
  - <sup>42</sup> H.-Q. Zhou and J.P. Barjaktarevič, J. Phys. A: Math. Theor. **41**, 412001 (2008); H.-Q. Zhou, R. Orús, and G. Vidal, Phys. Rev. Lett. **100**, 080601 (2008).